

Substructure of a Rubidium-Ion-Exchanged Form of the Silicate Nepheline Hydrate I

STAFFAN HANSEN AND LARS FÄLTH

Inorganic Chemistry 2, Chemical Center, University of Lund, P.O. Box 124, S-221 00 Lund, Sweden

Received March 21, 1984; in revised form May 18, 1984

X-Ray structure analysis of a nepheline hydrate I crystal, Rb⁺-exchanged at 80°C, was performed making use only of the main diffractions. The resulting substructure was found to be orthorhombic with $a = 8.0802(8)$, $b = 15.259(2)$, $c = 5.1584(5)$ Å, $V = 636.0$ Å³, space group $Pnm2_1$. Fourier and least-squares techniques gave the residuals $R = 0.048$ and $R_w = 0.058$, and a tentative formula of $RbNa_2Al_3Si_3O_{12} \cdot H_2O$ ($Z = 2$, $D_c = 2.65$ g cm⁻³). Tetrahedral distances were consistent with Al,Si alternation in the framework. Of the channel species, Na(1) and Na(2) were found not to be exchangeable at the current temperature. These sodium atoms are located in the small cages, formed by 6-rings of O atoms which connect the 8-ring channels parallel to c into two-dimensional pore systems. In the larger tunnels the replacement was complete and these contain a Rb⁺ ion and probably a water molecule in symmetry-related positions. According to this model, Rb⁺ coordinates four oxygens of an 8-ring and two water molecules, with Rb-O distances in the range 2.81-3.36 Å. Additional O atoms are found at greater distances. © 1984 Academic Press, Inc.

Introduction

Nepheline hydrate I (NHI) is a microporous framework silicate with the composition $Na_3Al_3Si_3O_{12} \cdot 2H_2O$ (1). The structures produced by the treatment of NHI with aqueous solutions of potassium chloride and cesium chloride, are the subject of discussion in Refs. (2, 3). Most of the alkali-exchanged forms of NHI exhibit superstructures which are apparently due to the ordering of cations and water molecules on alternative structural sites. Formation of often complicated superstructures, as a result of changes in temperature or composition is a common phenomena in many natural tektosilicate materials like *e*-plagioclase (4), nepheline (5), nosean (6), and cancrinite (7). In diffraction experiments,

these superstructures are manifested by commensurate or incommensurate satellite reflections. NHI should be a suitable substance for the study of these effects since it lacks Si,Al disorder. The structural complexities of many tektosilicates are in part caused by the simultaneous ordering of cations etc. in the framework pores and of Si,Al in the tetrahedral frame. This paper reports the average structure of a rubidium-exchanged nepheline hydrate I (RbNHI) as a first step in the investigation of this structure.

Experimental

Crystals of NHI, produced by the hydrothermal reaction of a silicate glass and NaOH at 200°C, were ion-exchanged with

TABLE I
COLLECTION AND REDUCTION OF X-RAY
INTENSITIES. DATA ON THE FINAL REFINEMENT

Temperature	20°C
Radiation	MoK α (graphite monochromator)
2 θ interval	6–70°
ω – 2 θ scan width, $\Delta 2\theta$	2.4° + $\alpha_1\alpha_2$ splitting
Scan rate	1.0–29.3° min ⁻¹
Total background time	0.75 \times scan time
Linear absorption coefficient, μ	4.72 mm ⁻¹
Range of transmission factors	0.63–0.78
Number of reflections measured	1670
Number of reflections with zero weight	911
Number of reflections in final refinement, m	759
Number of parameters refined, n	92
$R = \Sigma F_o - F_c / \Sigma F_o $	0.048
$R_w = [\Sigma w(F_o - F_c)^2 / \Sigma w F_o ^2]^{1/2}$	0.058
$S = [\Sigma w(F_o - F_c)^2 / (m - n)]^{1/2}$	1.20

0.5 mole liter⁻¹ RbCl(aq) at 80°C. An NHI specimen weighing 0.03 g and with a cancrinite phase as an additional constituent, was exposed to 10 ml of salt solution for 2 periods of 1 week, the salt solution being renewed after the first week. As a result of the ion exchange many of the NHI crystals were fractured. An energy dispersive X-ray analysis undertaken with a Philips EM400 electron microscope disclosed the presence of Rb, Na, Al, Si, and minor amounts of Fe in the RbNHI crystals, which were identified by their morphology. Because of their low quality several crystals had to be examined on the Weissenberg camera, before a single crystal could be found. The crystals that were examined showed superlattice reflections along a^* . The superlattice spots of RbNHI were less diffuse than those of Cs⁺-exchanged nepheline hydrate I (CsNHI). Only the main spots were used in this study and an orthorhombic crystal lattice of dimensions: $a = 8.0802(8)$, $b = 15.259(2)$, $c = 5.1584(5)$ Å; $V = 636.0$ Å³, was determined by a least-squares refinement involving 39 angles measured by a Nicolet $P3m$ diffractometer, using a crystal of size $0.05 \times 0.11 \times 0.13$ mm. Since the Laue group was mmm and the systematic absences were:

$Ok\bar{l}$: $k + l = 2n + 1$, the structural symmetry $Pnm2_1$ was chosen instead of $Pnmm$; just as for CsNHI and KNHI. The space group $Pnm2_1$ is characterized in Table IV and there is a simple relationship to the symmetry of NHI, which is $Pna2_1$. The values of the parameters used in the subsequent collection, and reduction of the intensity data, are given in Table I. One set of independent diffractions was monitored and there was only a random intensity variation in the 2 2 1 reflection, which was checked after every 100 reflections. The material was corrected for Lorentz, polarization, and absorption effects, and intensities with $I < 3\sigma(I)$ were given zero weight in the following refinements.

Structure Refinement

After a least-squares refinement that minimized the quantity $\Sigma w(|F_o| - |F_c|)^2$ and included the tetrahedral framework atoms of NHI, a difference Fourier synthesis revealed three new electron density peaks, located in the pores of the framework. Two of those were identified as unexchanged sodium ions (Na(1), Na(2)) while the third was considered to be a half-occupied Rb⁺ site (Rb(1)). The third peak was positioned near the center of an 8-ring tunnel of O atoms, but in contrast to the case of KNHI it was not possible, even by close inspection, to detect any splitting of the peak in the difference electron density maps, into two overlapping peaks. The structure was first refined to $R = 0.074$ with isotropic displacement factors. Then the occupancy factors (g 's) of Na(1), Na(2), and Rb(1) were also released with the results: 0.48(1), 0.50(1), and 0.557(9), respectively. The correlation coefficients between g and B for the three atoms were all approximately 0.7. Full occupancy of Na(1) and Na(2), which were in twofold special positions, required $g = 0.50$. Rb(1) was in the general fourfold position, but g could not exceed 0.5 because of

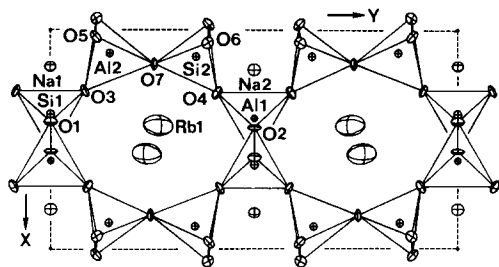


FIG. 1. Structure of Rb⁺-exchanged nepheline hydrate I projected along *c* with displacement ellipsoids of 50% probability. W(1) occupies the same position as Rb(1).

the 2.8-Å separation of Rb(1) positions generated by a twofold screw axis along *c*. Consequently all three *g*'s were again fixed at 0.5 and a residual index of $R = 0.054$ was obtained with anisotropic displacement, except for Si and Al. In the succeeding difference map there was residual electron density around the Rb(1) site, with a maximum height of $1.8 e \text{ \AA}^{-3}$. At this stage it was assumed that, in addition to Rb(1), a water molecule (W(1)) with $g = 0.50$ occupied the same position, within the experimental resolution of 0.62 Å. With this addition and weights calculated as $w^{-1} = \sigma^2(|F_0|) + (0.025|F_0|)^2 + 0.5$ convergence was finally reached (Table I). Reference (8) provided the necessary scattering factors and anomalous dispersion coefficients for neutral at-

TABLE II
POSITIONS, DISPLACEMENTS, AND OCCUPANCY FACTORS

Atom	<i>x</i>	<i>y</i>	<i>z</i>	B_{eq} (Å ²)	<i>g</i>
Rb(1)	0.4356(4)	0.2638(2)	0.780(2)	6.7(1)	0.50
Na(1)	0.1644(6)	0.00	0.781(2)	1.3(1)	0.50
Na(2)	0.1793(6)	0.50	0.784(2)	1.3(1)	0.50
Al(1)	0.4024(4)	0.50	0.251(2)	0.45(5) ^a	0.50
Al(2)	0.1015(3)	0.1457(1)	0.245(1)	0.61(4) ^a	1.0
Si(1)	0.3835(4)	0.00	0.25	0.70(5) ^a	0.50
Si(2)	0.1172(2)	0.3574(1)	0.243(2)	0.62(4) ^a	1.0
O(1)	0.418(1)	0.00	0.560(2)	1.1(2)	0.50
O(2)	0.445(1)	0.50	0.590(2)	1.0(2)	0.50
O(3)	0.2760(8)	0.0848(4)	0.168(2)	1.2(2)	1.0
O(4)	0.2847(8)	0.4089(4)	0.165(2)	1.3(2)	1.0
O(5)	0.0288(8)	0.1114(5)	0.546(2)	1.3(2)	1.0
O(6)	0.0566(8)	0.3860(4)	0.533(2)	1.2(1)	1.0
O(7)	0.1521(7)	0.2551(4)	0.219(2)	1.3(1)	1.0
W(1)	0.4356(4)	0.2638(2)	0.780(2)	6.7(1)	0.50

^a B_{iso} .

oms. In the last difference map the highest peaks were still close to Rb(1) and the maximum height was $1.3 e \text{ \AA}^{-3}$. Tables II and III present structural parameters, while Table IV gives some distances and angles.

Discussion

The RbNHI structure was refined as $\text{Rb}_{1.0}\text{Na}_{2.0}\text{Al}_3\text{Si}_3\text{O}_{12} \cdot \text{H}_2\text{O}$ ($Z = 2$), a composition which gave a calculated density of 2.65 g cm^{-3} . Figure 1 gives a projection of the structure.

TABLE III
ANISOTROPIC DISPLACEMENT FACTORS OF THE FORM $\exp(-\beta_{11} \cdot h^2 - \dots - 2\beta_{12} \cdot hk - \dots)$

Atom	β_{11}	β_{22}	β_{33}	β_{12}	β_{13}	β_{23}
Rb(1), W(1)	0.0182(5)	0.0108(2)	0.051(2)	0.0012(3)	0.0030(7)	-0.0074(7)
Na(1)	0.0041(6)	0.0017(2)	0.012(3)	0.0	-0.001(1)	0.0
Na(2)	0.0054(7)	0.0019(2)	0.006(3)	0.0	-0.0004(11)	0.0
O(1)	0.003(1)	0.0022(4)	0.005(3)	0.0	-0.002(2)	0.0
O(2)	0.0012(9)	0.0022(4)	0.006(3)	0.0	-0.0005(16)	0.0
O(3)	0.0059(8)	0.0008(2)	0.012(3)	0.0012(4)	0.002(1)	0.0011(6)
O(4)	0.0063(8)	0.0012(2)	0.011(3)	-0.0013(4)	0.002(1)	-0.0003(7)
O(5)	0.0054(9)	0.0014(3)	0.011(3)	0.0013(4)	0.003(1)	0.0014(6)
O(6)	0.0051(8)	0.0016(3)	0.007(2)	-0.0003(4)	0.001(1)	-0.0012(6)
O(7)	0.0062(6)	0.0004(2)	0.018(2)	-0.00003(33)	0.001(1)	-0.0004(9)

TABLE IV
 DISTANCES (Å) AND ANGLES (°)

(a) Tetrahedral framework				
Al(1)–O(4)	1.742(7)	Al(2)–O(7)	1.723(6)	
Al(1)–O(4 ^{vii})	1.742(7)	Al(2)–O(3)	1.735(7)	
Al(1)–O(1 ^{xii})	1.752(12)	Al(2)–O(5)	1.741(11)	
Al(1)–O(2)	1.781(17)	Al(2)–O(6 ^{xiii})	1.749(9)	
Mean	1.754	Mean	1.737	
O(4)–Al(1)–O(4 ^{vii})	105.8(5)	O(5)–Al(2)–O(6 ^{xiii})	103.2(4)	
O(1 ^{xii})–Al(1)–O(4)	107.9(6)	O(3)–Al(2)–O(6 ^{xiii})	107.6(4)	
O(1 ^{xii})–Al(1)–O(4 ^{vii})	107.9(6)	O(3)–Al(2)–O(7)	107.9(3)	
O(2)–Al(1)–O(4)	110.9(6)	O(3)–Al(2)–O(5)	108.5(4)	
O(2)–Al(1)–O(4 ^{vii})	110.9(6)	O(6 ^{xiii})–Al(2)–O(7)	113.1(4)	
O(1 ^{xii})–Al(1)–O(2)	113.2(5)	O(5)–Al(2)–O(7)	116.0(5)	
Mean	109.4	Mean	109.4	
Si(1)–O(3)	1.614(6)	Si(2)–O(7)	1.591(6)	
Si(1)–O(3 ⁱ)	1.614(6)	Si(2)–O(4)	1.616(7)	
Si(1)–O(2 ^{xiv})	1.614(9)	Si(2)–O(5 ^{xiii})	1.627(10)	
Si(1)–O(1)	1.622(11)	Si(2)–O(6)	1.635(12)	
Mean	1.616	Mean	1.617	
O(3)–Si(1)–O(3 ⁱ)	106.5(5)	O(5 ^{xiii})–Si(2)–O(6)	106.0(4)	
O(2 ^{xiv})–Si(1)–O(3)	109.2(3)	O(4)–Si(2)–O(5 ^{xiii})	108.0(6)	
O(2 ^{xiv})–Si(1)–O(3 ⁱ)	109.2(3)	O(4)–Si(2)–O(7)	108.1(4)	
O(1)–Si(1)–O(3)	110.6(4)	O(4)–Si(2)–O(6)	110.5(5)	
O(1)–Si(1)–O(3 ⁱ)	110.6(4)	O(5 ^{xiii})–Si(2)–O(7)	111.6(5)	
O(1)–Si(1)–O(2 ^{xiv})	110.7(5)	O(6)–Si(2)–O(7)	112.6(6)	
Mean	109.5	Mean	109.5	
Al(1)–O(2)–Si(1 ^{xv})	131.9(6)			
Al(1 ^{xv})–O(1)–Si(1)	134.3(7)			
Al(2)–O(5)–Si(2 ⁱⁱ)	135.5(5)			
Al(2 ⁱⁱ)–O(6)–Si(2)	135.9(5)	Range of distance	3.102(11)–	
Al(1)–O(4)–Si(2)	141.4(7)	Al–Si:	3.233(3)	
Al(2)–O(3)–Si(1)	143.8(6)	Mean distance		
Al(2)–O(7)–Si(2)	154.5(4)	Al–Si:	3.158	
Mean	140.7			
(b) NaO₇ polyhedra				
Na(1)–O(1)	2.35(1)	Na(2)–O(2)	2.37(1)	
–O(5)	2.36(1)	–O(6)	2.39(1)	
–O(5 ⁱ)	2.36(1)	–O(6 ^{vii})	2.39(1)	
–O(3 ^{iv})	2.55(1)	–O(4 ^{iv})	2.55(1)	
–O(3 ^{vi})	2.55(1)	–O(4 ^{viii})	2.55(1)	
–O(6 ⁱⁱ)	2.813(9)	–O(5 ⁱⁱ)	2.75(1)	
–O(6 ^{ix})	2.813(9)	–O(5 ⁱⁱⁱ)	2.75(1)	
(c) Environment of Rb⁺				
Rb(1)–W(1 ^{xi})	2.81(1)	Rb(1)–O(7 ^{xi})	3.358(6)	
–W(1 ^{xi})	2.81(1)	–O(4 ^{xi})	3.523(7)	
–O(4 ^{iv})	3.214(9)	–O(3 ^{iv})	3.625(9)	
–O(7 ^{iv})	3.23(1)	–O(7)	3.69(1)	
–O(3 ^{xi})	3.331(7)	–O(2)	3.735(5)	
(d) Water molecule				
W(1)–O(4 ^{iv})	3.214(9)	O(3 ^{xi})–W(1)–O(4 ^{iv})	83.9(2)	
–O(7 ^{iv})	3.23(1)	O(3 ^{xi})–	–O(7 ^{iv})	130.3(3)
–O(3 ^{xi})	3.331(7)	O(3 ^{xi})–	–O(7 ^{xi})	49.4(2)
–O(7 ^{xi})	3.358(6)	O(4 ^{iv})–	–O(7 ^{iv})	47.5(2)
		O(4 ^{iv})–	–O(7 ^{xi})	119.5(2)
		O(7 ^{iv})–	–O(7 ^{xi})	140.0(4)

TABLE IV—Continued

Symmetry code	
(None) x, y, z^a	(ix) $-x, -\frac{1}{2} + y, \frac{1}{2} + z$
(i) $x, -y, z^a$	(x) $1 - x, \frac{1}{2} - y, -\frac{1}{2} + z$
(ii) $-x, \frac{1}{2} - y, \frac{1}{2} + z^a$	(xi) $1 - x, \frac{1}{2} - y, \frac{1}{2} + z$
(iii) $-x, \frac{1}{2} + y, \frac{1}{2} + z^a$	(xii) $1 - x, \frac{1}{2} + y, -\frac{1}{2} + z$
(iv) $x, y, 1 + z$	(xiii) $-x, \frac{1}{2} - y, -\frac{1}{2} + z$
(v) $x, -y, 1 + z$	(xiv) $1 - x, -\frac{1}{2} + y, -\frac{1}{2} + z$
(vi) $x, 1 - y, z$	(xv) $1 - x, \frac{1}{2} + y, \frac{1}{2} + z$
(viii) $x, 1 - y, 1 + z$	(xvi) $1 - x, -\frac{1}{2} + y, \frac{1}{2} + z$

^a Equivalent positions of space group $Pnm2_1$.

^b Rb–O distances less than the shortest Rb–T distance are included.

Inspection of the crystal data of NHI and RbNHI revealed that the change in composition was accompanied by the following changes in the lattice constants: $\Delta a = -1.6\%$, $\Delta b = +1.6\%$, $\Delta c = -1.2\%$, and $\Delta V = -1.3\%$. This means that the framework distortion is of the same type as that in KNHI and CsNHI, but that the magnitudes are greater for RbNHI. This could be one cause of the low crystal quality of RbNHI. As can be deduced from the T–O distances in Table IVa there was again a high degree of Si,Al ordering in the framework tetrahedra. It was difficult to recognize any enlargement of the tetrahedra which could be attributed, with any certainty, to substitution by Fe(III), though a small amount of iron was indicated by the qualitative chemical analysis.

The arrangement of channel species in RbNHI, demonstrated that the Na(1) and Na(2) ions were locked in and were difficult to remove by Rb⁺ exchange at 80°C. The corresponding Na⁺ ions in KNHI and CsNHI exhibit a similar behavior. These Na⁺ ions coordinate seven framework O atoms (Table IVb) and are accommodated in the smaller cages limited by 6-rings that connect the 8-ring tunnels along c into two-dimensional pore systems in the bc plane. In the 8-ring channels, the original extra framework species (Na⁺, 2H₂O) were replaced by Rb⁺ and probably H₂O. The existence of the water molecule, W(1) was supported by (1) lower R values, (2) $g > 0.5$

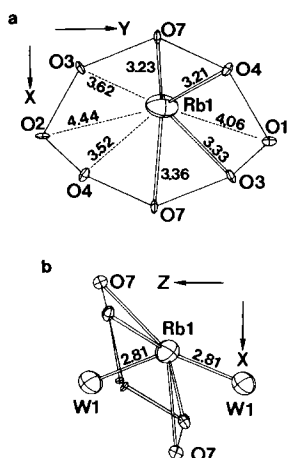


FIG. 2. Environment of Rb(1) with displacement ellipsoids drawn at the 50% probability level and distances given in Ångströms. (a) *ab* projection, (b) *ac* projection.

for Rb(1), (3) residual difference electron density around Rb(1), and (4) improved coordination for Rb(1). As can be seen in Figs. 2a and b, Rb(1) is situated near the center of an oval 8-ring of framework O atoms, although the Rb⁺ ion is somewhat displaced out of the plane of the ring. K(1) in KNHI is in a similar position but it is found approximately in the plane of the ring, a difference which is explained by the smaller size of the K⁺ ion. Six Rb–O distances of less than 3.36 Å have been emphasized in the figures, but this number is rather arbitrary since Table IVc indicates four more oxygens at 3.52–3.74 Å. If no water molecules were present, Rb(1) would, as before, coordinate at least four of the 8-ring oxygens at reasonable distances while O(7), which belongs to another 8-ring, is as far away as 3.69 Å. This O(7) atom is used in CsNHI to complete the coordination sphere of Cs(1) which is situated in an analogous site. Rubidium atoms which only coordinate framework O atoms of a single 8-

ring are exclusively found in dehydrated zeolites like Rb⁺-exchanged zeolite A (9) where four of the eight oxygens are at distances of 3.2 Å and the rest at 3.7 Å, from the ion designated Rb(2). Another example is dehydrated Rb–mordenite (10) where RbIV has six of the 8-ring oxygens at 3.08 and 3.30 Å and the last two at 3.75 Å. Conventional Rb-containing tektosilicates have more spherical oxygen arrangements around the Rb atoms. For example, synthetic sanidine, RbAlSi₃O₈ (11) with CN = 9 and Rb–O distances of 2.95–3.17 Å and the phase RbAlSiO₄ (12) which has 11 oxygens at 2.91–3.54 Å from Rb⁺. Table IVd shows that the framework of RbNHI provides an environment suitable for the water molecule W(1). In order to confirm and precisely locate the proposed water molecule by X-ray methods, the superlattice intensities must be taken into account.

References

1. S. HANSEN AND L. FÄLTH, *Zeolites* **2**, 162 (1982).
2. S. HANSEN AND L. FÄLTH, *J. Solid State Chem.* **55**, 225 (1984).
3. S. HANSEN AND L. FÄLTH, *Z. Kristallogr.* **164**, 79 (1983).
4. A. KUMAO, H. HASHIMOTO, H.-U. NISSEN, AND H. ENDOH, *Acta Crystallogr. Sect. A* **37**, 229 (1981).
5. J. D. C. MCCONNELL, *Amer. Mineral.* **66**, 990 (1981).
6. H. SCHULZ, *Z. Kristallogr.* **131**, 114 (1970).
7. H. D. GRUNDY AND I. HASSAN, *Canad. Mineral.* **20**, 239 (1982).
8. "International Tables for X-Ray Crystallography" (J. A. Ibers and W. C. Hamilton, Eds.), Vol. 4, Kynoch Press, Birmingham (1974).
9. J. J. PLUTH AND J. V. SMITH, *J. Amer. Chem. Soc.* **105**, 2621 (1983).
10. J. L. SCHLENKER, J. J. PLUTH, AND J. V. SMITH, *Mater. Res. Bull.* **13**, 77 (1978).
11. M. GASPERIN, *Acta Crystallogr. Sect. B* **27**, 854 (1971).
12. R. KLASKA AND O. JARCHOW, *Z. Kristallogr.* **142**, 225 (1975).